# Specificity of RCN1-Mediated Protein Phosphatase 2A Regulation in Meristem Organization and Stress Response in Roots[1][W][OA]

**Joshua J. Blakeslee[2], Hong-Wei Zhou[2,3], Jeffrey T. Heath[4], Kyle R. Skottke, Jorge A. Rodriguez Barrios, Su-Yang Liu[5], and Alison DeLong***

Department of Molecular Biology, Cell Biology, and Biochemistry, Brown University, Providence, Rhode Island 02912

Protein dephosphorylation by the serine/threonine protein phosphatase 2A (PP2A) modulates a broad array of cellular functions. PP2A normally acts as a heterotrimeric holoenzyme complex comprising a catalytic subunit bound by regulatory A and B subunits. Characterization of the regulatory A subunit isoforms (ROOTS CURL IN NAPHTHYLPHTHALAMIC ACID1 [RCN1], PP2AA2, and PP2AA3) of *Arabidopsis thaliana* PP2A has shown that RCN1 plays a primary role in controlling root and hypocotyl PP2A activity in seedlings. Here we show that hypocotyl and root growth exhibit different requirements for RCN1-mediated regulation of PP2A activity. Roots of *rcn1* mutant seedlings exhibit characteristic abnormalities in cell division patterns at the root apical meristem, as well as reduced growth under ionic, osmotic, and oxidative stress conditions. We constructed chimeric A subunit genes and found that restoration of normal root tip development in *rcn1* plants requires both regulatory and coding sequences of *RCN1*, whereas the hypocotyl elongation defect of *rcn1* plants can be complemented by either *RCN1* or *PP2AA3* transgenes. Furthermore, the *RCN1* and *PP2AA3* proteins exhibit ubiquitous subcellular localization patterns in seedlings and both associate with membrane compartments. Together, these results show that RCN1-containing PP2A has unique functions that cannot be attributed to isoform-specific expression and localization patterns. Postembryonic *RCN1* function is required to maintain normal auxin distribution and stem cell function at the root apex. Our data show that *RCN1*-regulated phosphatase activity plays a unique role in regulating postembryonic root development and stress response.

Regulated dephosphorylation by protein phosphatases (PPs) has emerged as a universal control mechanism in physiology and development. Important roles have been identified for a variety of PP species in plants. For instance, several PP2C enzymes negatively regulate abscisic acid (ABA) response (for review, see Schweighofer et al., 2004; Yoshida et al., 2006), whereas other PP2Cs modulate wound signaling, stress signaling, and meristem development (Stone et al., 1998; Song and Clark, 2005; Schweighofer et al., 2007). Similarly, distinct dual-specificity phosphatases regulate carbohydrate metabolism (Kerk et al., 2006; Niittyla et al., 2006; Sokolov et al., 2006) and oxidative, saline, and genotoxic stress tolerance (Ulm et al., 2002; Lee and Ellis, 2007). PP2A, which constitutes an abundant population of oligomeric enzymes, plays crucial roles in the regulation of growth and development. Altered PP2A activity in plants has been linked to defects in hormone homeostasis and signaling, defense responses, cell division, morphogenesis, and reproduction (for review, see DeLong, 2006). Analysis of Arabidopsis (*Arabidopsis thaliana*) PP2A mutants suggests that important substrates for PP2A include proteins that control microtubule dynamics (Camilleri et al., 2002) and components of the auxin transport apparatus (Rashotte et al., 2001; Shin et al., 2005; Michniewicz et al., 2007).

The predominant form of PP2A is a heterotrimeric complex containing a catalytic (C) subunit, a scaffolding/regulatory (A) subunit, and a regulatory (B) subunit (Janssens and Goris, 2001). Combinatorial diversity of these heterotrimers enhances the versatility of the enzyme complex. The C and A subunits are abundant, ubiquitous, and highly conserved, whereas B subunits exhibit more specific expression patterns and are encoded by several unrelated gene families. Localization and substrate specificity of PP2A action are controlled largely through the effects of bound A and B subunits.

[1] This work was supported by the National Science Foundation (grant no. IOB–0446039). The work was partially supported by the U.S. Department of Agriculture Cooperative State Research, Education, and Extension Service (award no. 2007–35304–18418 to J.J.B.), and K.R.S. was partially supported by the National Institutes of Health predoctoral training program (grant no. GM007601).

[2] These authors contributed equally to the article.

[3] Present address: Neurology Research, St. Elizabeth's Medical Center, Boston, MA 02135.

[4] Present address: Department of Automated Biotechnology, Merck and Company, North Wales, PA 19454.

[5] Present address: Department of Microbiology, Immunology and Molecular Genetics, University of California Los Angeles, Los Angeles, CA 90024.

* Corresponding author; e-mail alison_delong@brown.edu.

The author responsible for distribution of materials integral to the findings presented in this article in accordance with the policy described in the Instructions for Authors (www.plantphysiol.org) is: Alison DeLong (alison_delong@brown.edu).

[W] The online version of this article contains Web-only data.

[OA] Open Access articles can be viewed online without a subscription.

www.plantphysiol.org/cgi/doi/10.1104/pp.107.112995

The regulatory A subunit comprises 15 imperfect repeats of the α-helical HEAT (huntingtin, elongation factor 3, A subunit, and TOR proteins; Andrade and Bork, 1995). The carboxy-terminal repeats bind the catalytic subunit, and the amino-terminal repeats bind the B subunit. Both binding interactions employ a hydrophobic binding interface formed by short and variable loops located in the center of each HEAT repeat (see Supplemental Fig. S1A; Ruediger et al., 1994; Xing et al., 2006). The A subunit performs at least three crucial regulatory functions. First, binding of the A subunit alters the kinetic properties of the C subunit (Price and Mumby, 2000). Second, A subunit binding also allows interaction of C subunits with the diverse B subunits involved in targeting PP2A function to its physiological targets (Ruediger et al., 1994). Third, recent work indicates that A subunit binding is required for acquisition of the fully activated C subunit conformation (Hombauer et al., 2007). A single regulatory A subunit isoform appears to suffice in rice (*Oryza sativa*) and maize (*Zea mays*), as well as in several fungi (van Zyl et al., 1992; Kinoshita et al., 1996; Yu et al., 2001), whereas mammalian systems rely on two differentially expressed and functionally distinct isoforms (Zhou et al., 2003; Sablina et al., 2007).

The Arabidopsis genome encodes three functionally distinct A subunit isoforms, ROOTS CURL IN NAPHTHYLPHTHALAMIC ACID1 (RCN1), PP2AA2, and PP2AA3 (Slabas et al., 1994; Zhou et al., 2004), with RCN1 alone acting as a key positive regulator of PP2A activity in seedlings. Biochemical and physiological analyses show reduced PP2A enzymatic activity in *rcn1* plants, and *rcn1* mutant phenotypes result from loss of PP2A activity in vivo (Deruère et al., 1999; Rashotte et al., 2001; Kwak et al., 2002; Larsen and Cancel, 2003). Basipetal auxin transport is increased in hypocotyls and roots of *rcn1* seedlings, resulting in altered gravitropic response in both organs (Rashotte et al., 2001; Shin et al., 2005; Muday et al., 2006). *RCN1* also functions as a transducer of ABA signals, acting upstream of ABA-induced increases in cytosolic $Ca^{2+}$, but downstream of the PP2C ABI1 (Kwak et al., 2002), and as a negative regulator of ethylene synthesis (Larsen and Chang, 2001; Muday et al., 2006). Additional data suggest a negative regulatory role for *RCN1* in ethylene signaling in shoots (Larsen and Chang, 2001; Larsen and Cancel, 2003).

The abnormal phenotypes of *rcn1* mutant plants show that RCN1-containing PP2A species perform regulatory functions that are not mediated by complexes containing the other regulatory A subunit isoforms. Despite gene expression patterns that overlap with that of *RCN1*, loss of *PP2AA2* and/or *PP2AA3* function does not significantly alter phosphatase inhibitor sensitivity or produce dramatic mutant phenotypes (Zhou et al., 2004). However, plants carrying a *pp2aa2* or *pp2aa3* mutation in combination with *rcn1* exhibit severe morphological and developmental abnormalities including arrested primary root growth (Zhou et al., 2004; Michniewicz et al., 2007). Degeneration of the primary root apical meristem in *rcn1 pp2aa2* and *rcn1 pp2aa3* seedlings appears to be caused by loss of auxin signaling, and is associated with relaxed or reversed localization of PIN-FORMED (PIN) proteins in embryos and seedling roots (Michniewicz et al., 2007). The radial cell and organ expansion phenotypes exhibited by these seedlings are similar to those of seedlings grown in the presence of high doses of phosphatase inhibitors, and therefore demonstrate the effect of drastic loss of PP2A activity (Rashotte et al., 2001; Shin et al., 2005; Muday et al., 2006).

We asked whether we could distinguish between functions that specifically require the RCN1 protein sequence and functions that are sensitive to overall A subunit dosage but insensitive to isoform specificity. To address this question, we undertook functional analyses in vivo, using constructs that carry regulatory and coding sequences from different A subunit-encoding genes to rescue *rcn1* defects in seedling hypocotyls and in roots. The reduced hypocotyl elongation phenotype of *rcn1* can be rescued by *PP2AA3* constructs; however, restoration of wild-type root tip organization requires both promoter and coding sequences of *RCN1*. Thus hypocotyl growth is sensitive to A subunit gene dosage but relatively insensitive to isoform specificity, whereas regulation of root growth requires PP2A complexes containing the RCN1 regulatory subunit. We show that loss of *rcn1* alone causes increased sensitivity to a broad panel of stress treatments and compromises the maintenance of organized stem cell populations. Inhibition of phosphatase activity in seedlings is sufficient to recapitulate the *rcn1* phenotype at the root apex, indicating that RCN1-mediated phosphatase regulation is required postembryonically for normal meristem function. Our data suggest that the RCN1 protein specifically mediates interactions targeting PP2A to substrates required for root stress response and meristem function.

## RESULTS

### Arabidopsis *RCN1-YFP* Fusions Retain Biological Activity

To facilitate our investigation of the biological specificity determinants for *RCN1* function in plants, we constructed amino- and carboxy-terminal fusions of *RCN1* with the yellow fluorescent protein (YFP) reporter (see "Materials and Methods"). We first tested cDNA fusions for biological activity using a complementation assay in the yeast PP2A regulatory A subunit mutant, *tpd3-1*. The *tpd3-1* mutation confers temperature sensitivity and slow growth phenotypes that are complemented by the *RCN1* cDNA (Garbers et al., 1996), as well as sensitivity to stress conditions such as nitrogen starvation and osmotic stress (Santhanam et al., 2004). RCN1-YFP amino- and carboxy-terminal fusion proteins were expressed under control of the constitutive alcohol dehydrogenase promoter (Ammerer,

1983). Both constructs rescued growth of *tpd3* mutant at high temperature, indicating that the fusion proteins are competent to regulate the yeast PP2A complex (Fig. 1A). YFP fluorescence was detected in yeast cells carrying *RCN-YFP* and *YFP-RCN* (Fig. 1B) and full-length fusion proteins were detected by anti-GFP (Fig. 1C) and anti-RCN1 (see Supplemental Fig. S1B) antibodies. Although the predicted molecular masses of the two fusion proteins were nearly identical (94 kD), the RCN1-YFP fusion consistently exhibited a slightly slower SDS-PAGE migration when extracted from both yeast and plant cells (see below). The *RCN1-YFP* fusion also complemented the *tpd3* stress sensitivity phenotype and rescued growth in the presence of salt (Fig. 1D) and sorbitol (data not shown). Thus fusion of YFP to either terminus does not impair the regulatory A subunit function of RCN1 in yeast.

### *YFP-RCN1* and *YFP-PP2AA3* Fusions Rescue the *rcn1* Hypocotyl Elongation Defect

To assay the biological activities of RCN1-YFP fusions in planta, we used a triple-template PCR (TT-PCR) template overlap strategy (Tian et al., 2004) to generate translational fusions in the context of the full-length genomic *RCN1* sequence (Fig. 2A). The resulting constructs carried 2.1 kb of genomic sequence upstream from the RCN1 transcript, the transcribed region (including introns), and 550 bp of downstream sequence. Both amino- and carboxy-terminal fusions were generated in the plant transformation vector pPZP221 (Hajdukiewicz et al., 1994) and transformed into *rcn1-1* mutant plants. To test for biological function, we assayed for complementation of the *rcn1* hypocotyl elongation defect (Fig. 2B). In families segregating for an $RCN_{pro}$:*YFP-RCN1* (*RYR*) or $RCN_{pro}$:*RCN1-YFP* (*RRY*) fusion, YFP fluorescence segregated with rescued hypocotyl elongation, whereas hypocotyl lengths of YFP-negative siblings matched those of the *rcn1* parent and the empty vector control. These data indicate that the YFP fusion proteins provide A subunit function in plants, as well as in yeast.

To allow direct comparison of the localization and biological activities of the RCN1 and PP2AA3 isoforms, we constructed equivalent YFP fusions to the *PP2AA3* cDNA (Fig. 2A). In one derivative the *YFP-PP2AA3* fusion remained under control of the *RCN1* promoter and 5′ untranslated region (*RYA*), while in the second construct the *RCN1* upstream sequences were replaced with a 1.2-kb fragment containing the *PP2AA3* leader (including a 312-bp intron), the intragenic region, and the predicted 5′ end of the next gene upstream (*AYA*). These constructs were designed to drive expression of the *YFP-PP2AA3* fusion in the *RCN1* and the *PP2AA3* domains, respectively. To avoid overexpression artifacts, we focused primarily on transformants carrying single-copy T-DNAs in the *rcn1* background. We assayed the ability of these fusions to complement the hypocotyl elongation defect of *rcn1* seedlings (Fig. 2C). Hypocotyl growth was fully restored in lines carrying

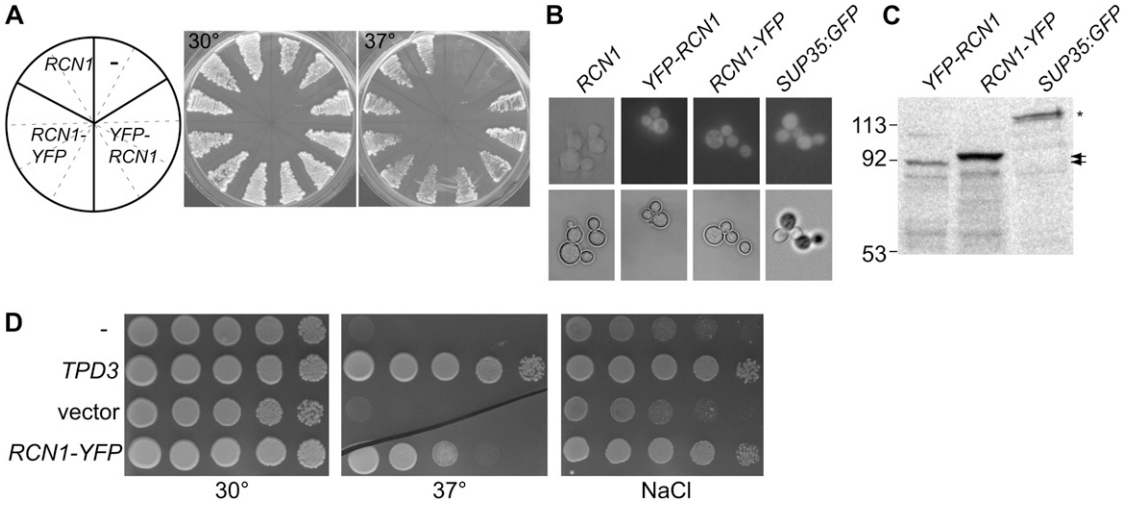


**Figure 1.** *RCN-YFP* fusions supply regulatory A subunit function in yeast. *RCN1-YFP* and *YFP-RCN1* fusions were expressed under control of the constitutive alcohol dehydrogenase promoter (Ammerer, 1983) in *tpd3-1* yeast cells (van Zyl et al., 1992). A, Transformants carrying *RCN-YFP* fusions, an *RCN1* construct, or the empty vector were streaked on duplicate YPD plates and incubated at 30°C or 37°C. The diagram at left indicates the construct carried by cells in the corresponding sectors on both plates. B, Cells carrying a native *RCN1* construct, *YFP-RCN1*, *RCN1-YFP*, or a *SUP35*:*GFP* fusion (Satpute-Krishnan and Serio, 2005) were grown to early log phase and mounted for differential interference contrast (bottom panels) or fluorescence (top panels) microscopy. C, Protein extracts of cells carrying the constructs indicated were subjected to SDS-PAGE and immunoblotting, using anti-GFP antibodies to detect the fusion proteins. The positions of the RCN1-YFP (black arrows) and SUP35:GFP (asterisk) proteins are indicated at right. D, Cells carrying the constructs indicated were grown in liquid culture and 10-fold serial dilutions were spotted on plates containing YPD medium or YPD plus 600 mM NaCl. YPD plates were incubated at 30°C or 37°C and YPD NaCl plates were incubated at 30°C.

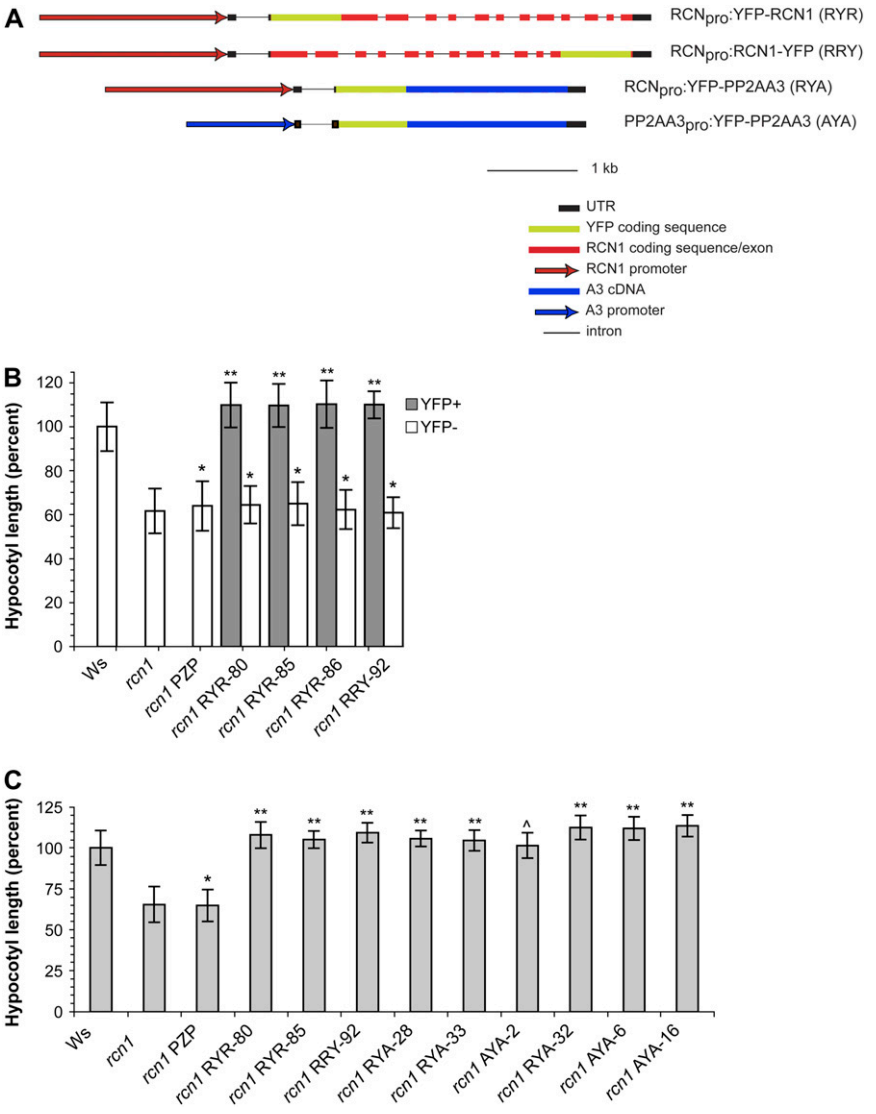


**Figure 2.** *RCN1* and *PP2AA3* fusions to *YFP* rescue hypocotyl elongation in the *rcn1* mutant. A, The *YFP* coding sequence was fused at the N- or C-terminal end of the *RCN1* gene (see "Materials and Methods") to generate in-frame fusions within the genomic *RCN1* sequence. In the $RCN_{pro}$*:YFP-PP2AA3* (*RYA*) construct, the *RCN1* coding sequence was replaced with the *PP2AA3* cDNA. The $PP2AA3_{pro}$*:YFP-PP2AA3* (*AYA*) construct was derived from *RYA* by substituting upstream sequences from *PP2AA3* for the *RCN1* regulatory region. All constructs were transformed into the *rcn1-1* mutant. B, Transformant families segregating for a single *YFP-RCN1* or *RCN1-YFP* transgene were scored for hypocotyl elongation and for YFP fluorescence after 5 d of growth in the dark. Values shown represent the average hypocotyl lengths for each class ($YFP^+$ or $YFP^-$) relative to the wild-type control (Ws). Error bars indicate SD; $n > 25$ for all controls; $n > 45$ for all segregating families. C, Homozygous transformant families carrying the transgene constructs indicated were scored for hypocotyl elongation after 5 d growth in the dark. Values shown represent the average hypocotyl lengths for each family relative to the wild-type control (Ws). Error bars indicate SD; $n > 25$ for all controls; $n > 45$ for all families carrying *YFP* fusion constructs. *rcn1* PZP is an *rcn1* transgenic line carrying the empty vector. Lines *rcn1* RYA-32 and *rcn1* AYA-6 each carry two copies of the fusion T-DNA, whereas line *rcn1* AYA16 carries three or more copies. All other lines carry the transgene construct in single copy. Levels of statistical significance as determined by Student's *t* test: *, $P > 0.15$ versus *rcn1* and $P < 10^{-6}$ versus Ws; **, $P < 10^{-30}$ versus *rcn1* and $P < 0.05$ versus Ws; ^, $P < 10^{-30}$ versus *rcn1* and $P > 0.8$ versus Ws.

the *YFP-PP2AA3* fusion under control of either the *RCN1* or *PP2AA3* promoter. Only a slight difference was observed between lines expressing *YFP-RCN* versus *YFP-PP2AA3* fusions, and this difference was eliminated in lines carrying *YFP-PP2AA3* in two or more copies (Fig. 2C; lines *rcn1 RYA-32*, *rcn1 AYA-6*, and *rcn1 AYA-16*). These data indicate that A subunit dosage is critical for supporting normal hypocotyl elongation, but RCN1-specific protein sequences are not strictly required for this activity.

### *RCN1*-Specific PP2A Regulation Maintains Root Tip Organization

We used confocal imaging to determine whether *rcn1* seedlings exhibit root tip disorganization phenotypes consistent with our hypothesis that increased basipetal auxin transport alters auxin distribution in *rcn1* roots. The normal root apical meristem exhibits a stereotypical arrangement of initial cells organized around a small population of quiescent center (QC) cells (for review, see Benfey and Scheres, 2000), and root tip architecture is disrupted by factors that alter the position or magnitude of an auxin concentration maximum in the root apex (Sabatini et al., 1999). Although wild-type roots maintained highly regular cell numbers and arrangement in the QC, columella initials, and root cap columella, *rcn1* seedlings showed disorganization indicating aberrant cell division patterns (Fig. 3). QC and cortical/endodermal initial cells were difficult to distinguish in *rcn1* seedlings and frequently failed to form a well-defined layer at the bottom of the stele. Columella cell files were abnormal in 68% of *rcn1* roots examined (versus 12% of wild-type roots), whereas columellar tiers were disrupted in 28% (versus 0 in the wild type; $n = 25$ for each genotype). In *rcn1* roots, cells formed irregular layers and cell numbers varied between different tiers. In several roots with three files of proper columella cells, a flanking file of lateral root cap cells appeared to have been recruited into a "shoulder"

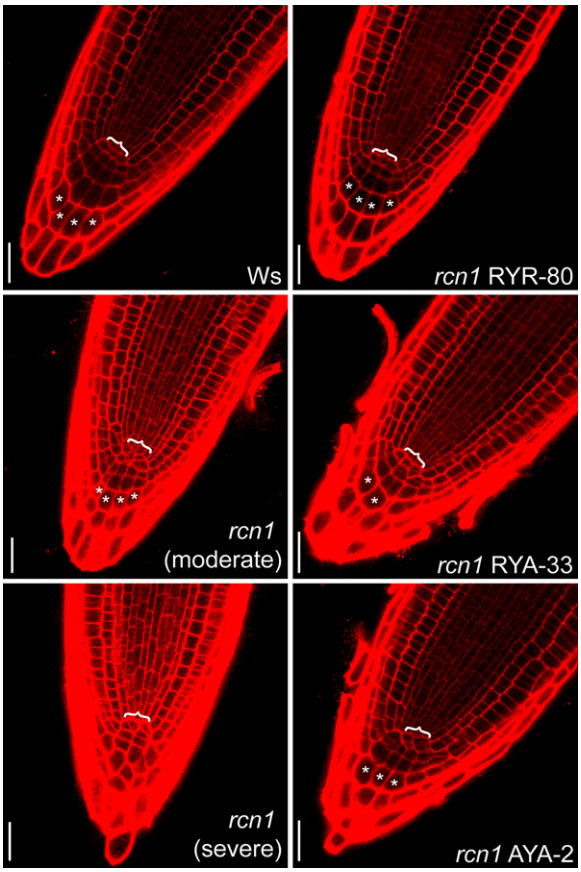


**Figure 3.** Isoform specificity of *RCN1* function in root tip organization. Median longitudinal sections of propidium iodide-stained 4-dpg root tips were captured using confocal laser microscopy, revealing normal meristem organization in wild-type (Ws) roots and highlighting the disorganization of columella and initial cells in *rcn1* root tips. Examples of moderate (*rcn1* moderate) and severe (*rcn1* severe) *rcn1* disorganization phenotypes are shown. The *YFP-RCN1* fusion restores wild-type morphology in *rcn1* plants carrying the *RYR* construct, whereas the *YFP-PP2AA3* fusions carried in *RYA* and *AYA* transformants fail to fully rescue the *rcn1* phenotype. Brackets indicate the region of the QC; asterisks indicate cells representative of clearly defined columellar cell files. Scale bars, 25 $\mu$m.

of the columella. All wild-type roots scored as abnormal exhibited regular files and tiers but had an abnormal number of cell files. As shown below, an independent *rcn1* allele in the Columbia (Col) genetic background showed similar defects in root tip organization.

We asked whether *YFP-RCN* and *YFP-PP2AA3* could rescue the abnormal morphology of *rcn1* root tips (Fig. 3). *RRY* and *RYR* lines exhibited identifiable QCs and clear restoration of columellar cell organization. In a representative *RYR* line, only 7% of roots exhibited an abnormal number of columellar files ($n = 15$). In contrast, columellar file number remained abnormal in roots of a representative *RYA* line (35%; $n = 23$) and a representative *AYA* line (26%; $n = 31$). Similarly, a regular columella initial cell layer was present in all wild-type and *RYR* root tips, with only 7% exhibiting an abnormal columella initial cell number, whereas 53% of *rcn1-1* roots, 30% of *RYA* roots, and 35% of *AYA* roots exhibited abnormal cell numbers in a columella initial cell layer that frequently was poorly defined. These data suggest that normal root tip organization specifically requires *RCN1* function; *YFP-PP2AA3* constructs that support normal hypocotyl elongation do not fully restore normal root growth. To ensure that fusion to YFP did not impair function of PP2AA3 protein in roots, we also assayed for rescue by a native *PP2AA3* construct (*PP2AA3*$_{pro}$:*PP2AA3*). The native *PP2AA3* construct also provided only weak complementation of *rcn1* root tip defects (data not shown). These data show that the requirements for A subunit function are more stringent in the root tip than in the hypocotyl, and suggest that increased *PP2AA3* dosage does not completely compensate for loss of *RCN1* function in the root tip.

Our earlier work on A subunit double mutants revealed severe root growth defects in *rcn1 pp2aa2* and *rcn1 pp2aa3* double mutants, but not in *pp2aa2 pp2aa3* double mutant seedlings (Zhou et al., 2004). We asked whether root growth in the *pp2aa2 pp2aa3* double mutant background was sensitive to decreased *RCN1* dosage. We assessed root tip morphology by visualizing amyloplasts in cleared root tips after staining for starch accumulation. As expected, starch staining revealed a highly regular arrangement of columellar cells in wild-type and *pp2aa2 pp2aa3* root tips, with clearly defined tiers and files of cells (see Supplemental Fig. S2). In *rcn1* root tips, columellar cell files and tiers often were irregular, indicating aberrant patterns of columella initial divisions. Overall columellar morphology in the *pp2aa2 pp2aa3 rcn1/+* mutant was similar to that observed in the *rcn1* background, with most roots exhibiting four poorly defined tiers of cells, and many lacking part or all of one columellar cell file. Consistent with a recent report (Michniewicz et al., 2007), columellar cell numbers were severely reduced and columellar files and tiers were difficult to identify in *rcn1 pp2aa2* and *rcn1 pp2aa3* root tips even at 4 d postgermination (dpg; see Supplemental Fig. S2). We conclude that *RCN1* function is required for normal root tip organization, and root growth is sensitive to *RCN1* dosage. Although *RCN1* becomes haploinsufficient in the *pp2aa2 pp2aa3* background, the heterozygous *RCN1* dose in *pp2aa2 pp2aa3 rcn1/+* mutants supports more normal development than a homozygous *PP2AA3* dose in the *rcn1 pp2aa2* double mutant.

### Normal Root Development Requires Postembryonic RCN1 Function

Abnormal embryogenesis in *rcn1 pp2aa2* and *rcn1 pp2aa3* plants (Zhou et al., 2004; Michniewicz et al., 2007) as well as enhancement of *pin1* and *pid* embryogenesis defects by *rcn1* (Zhou et al., 2004) indicate that *RCN1* is required for normal embryo development. To determine whether the root tip disorganization phenotype reflects an embryonic or a postembryonic requirement for RCN1 action, we asked whether chemical inhibition of PP activity in seedling roots

was sufficient to produce a phenocopy of *rcn1* root tip defects. We and others have previously used cantharidin to produce a phenocopy of *rcn1* in organ elongation, root curling, and basipetal auxin transport assays (Deruère et al., 1999; Rashotte et al., 2001; Shin et al., 2005), and other phosphatase inhibitors have been used to mimic the ethylene and ABA response phenotypes of *rcn1* (Kwak et al., 2002; Larsen and Cancel, 2003). We compared the root apex phenotypes of wild-type (Col) seedlings grown in the absence or presence of cantharidin with those of seedlings carrying *rcn1-6*, a T-DNA insertion allele (see "Materials and Methods"). RCN1 protein is undetectable in extracts of *rcn1-6* seedlings, and the gross hypocotyl and root phenotypes of *rcn1-6* seedlings are indistinguishable from those of the *rcn1-1* allele (data not shown). Poorly defined QCs and irregular columellar cell arrangements were observed in 86% of cantharidin-treated wild-type roots ($n = 24$), closely matching the defects exhibited by 94% of *rcn1-6* seedlings grown in the absence of inhibitor ($n = 18$; Fig. 4, A–D). Similar results were obtained with cantharidin-treated wild-type roots of another accession (Ws; data not shown). Thus the *rcn1* phenotype reflects a postembryonic requirement for normal PP2A regulation, as PP inhibition in seedlings is sufficient to disrupt normal root tip development.

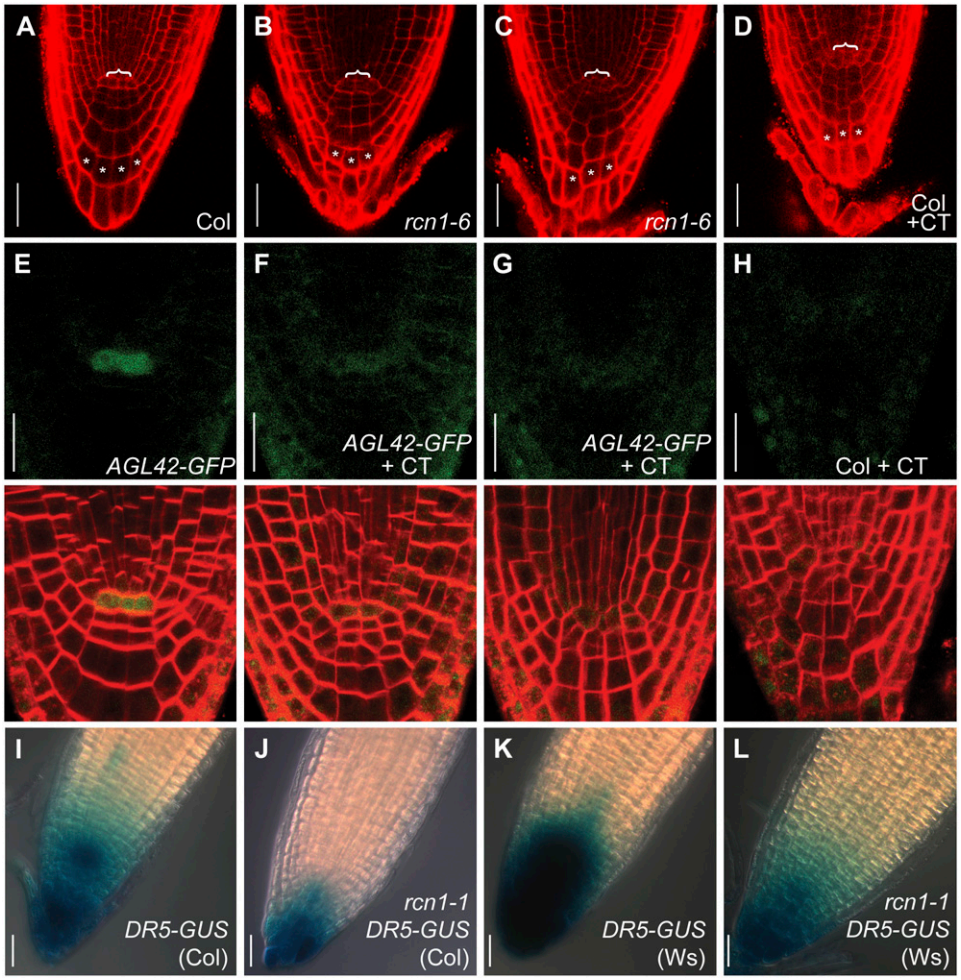


**Figure 4.** Postembryonic PP2A function maintains normal root tip development. Median longitudinal sections of propidium iodide-stained 4-dpg root tips were captured using confocal microscopy. One wild-type (A) and two representative *rcn1-6* mutant (B and C) root tips grown in the absence of cantharidin plus one wild-type root tip grown in the presence of 10 $\mu$M cantharidin (D) are shown. Cantharidin-treated wild-type roots show abnormalities around the QC (brackets) and reduced columellar cell file numbers matching those of *rcn1-6* mutant roots. Asterisks indicate cells representative of clearly defined columellar cell files. The *AGL42-GFP* reporter is expressed in QC cells in 4-dpg seedling roots (E), but its expression is severely reduced in seedlings grown in the presence of 10 $\mu$M cantharidin (F and G). Each FM4-64-stained seedling was scanned sequentially for GFP fluorescence (upper row) and FM4-64 fluorescence (overlay shown in lower row). Under the imaging conditions used, a low level of background fluorescence is detected in wild-type Col root tips grown in the presence of cantharidin (H). *DR5-GUS* reporter activity is reduced in roots of seedlings carrying the *rcn1-1* mutation in both the Col (I versus J) and Ws (K versus L) genetic backgrounds (see "Materials and Methods"). Scale bars, 25 $\mu$m (A–D and I–L) and 20 $\mu$m (E–H).

The disrupted columella organization observed in *rcn1* roots suggests abnormal function of the stem cell populations, particularly the columella initials and/or QC. We asked whether loss of phosphatase activity altered the expression of a molecular marker for QC identity. In roots the expression of a GFP reporter fused to the *AGL42* MADS-box gene is tightly restricted to the QC at 4 dpg (Nawy et al., 2005). Normal root tip organization and clear QC expression of *AGL42-GFP* were observed in 87% of untreated roots ($n = 23$; Fig. 4E). Strongly reduced expression of *AGL42-GFP* and abnormal root tip architecture were observed in 91% of cantharidin-treated seedling roots ($n = 23$; Fig. 4, F and G). In most cantharidin-treated roots, *AGL42-GFP* expression was reduced to background levels (Fig. 4, F–H). These observations are consistent with the hypothesis that loss of RCN1-regulated phosphatase activity compromises QC function. Reduced *AGL42-GFP* expression might be a consequence of decreased auxin accumulation at the root apex; however, we do not observe

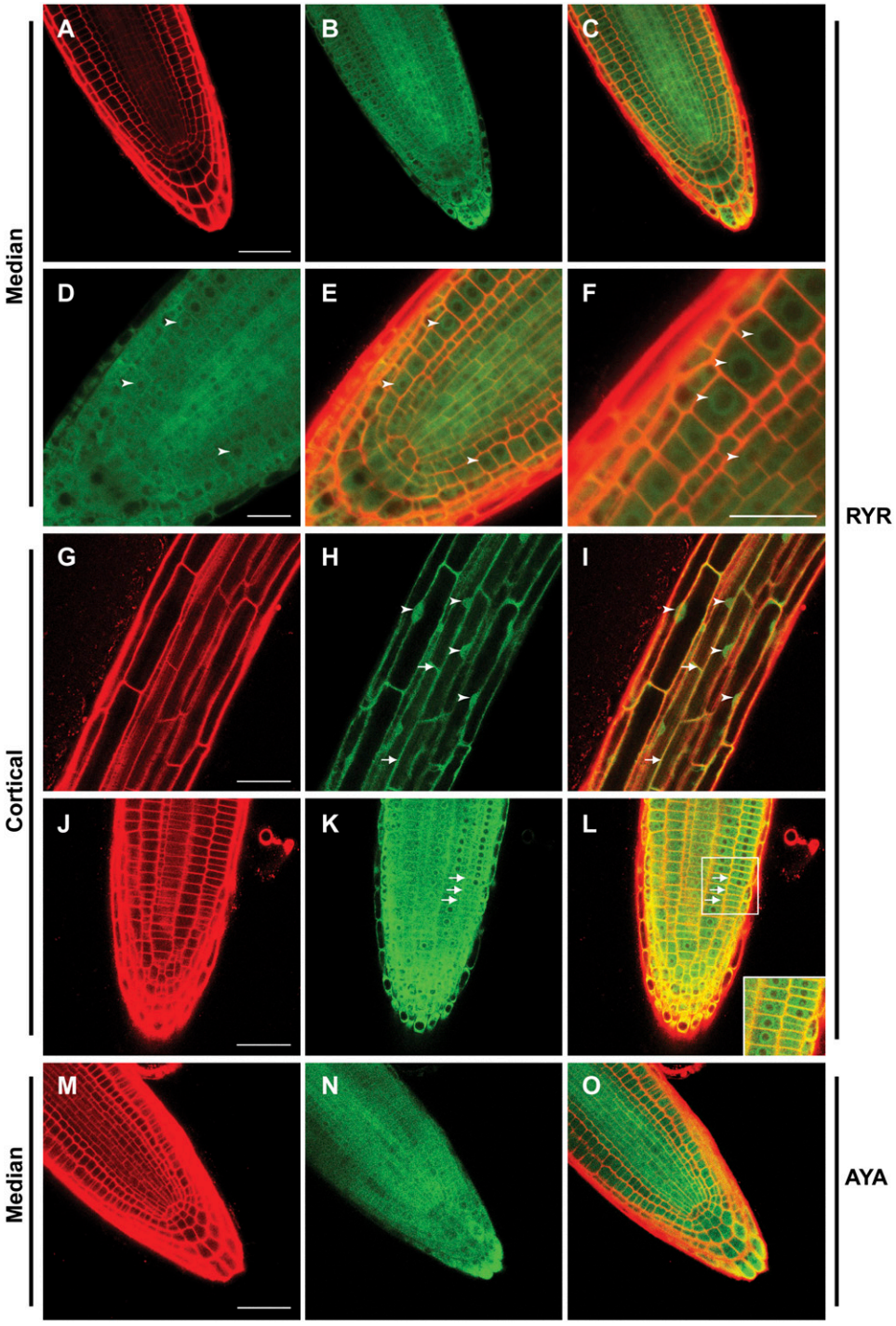


**Figure 5.** Abundance and localization of YFP-RCN1 protein in seedling roots. Confocal microscopy reveals that the YFP-RCN1 fusion protein is abundant in all cell layers of the root tip (A–C) and shows cytoplasmic and perinuclear (arrowheads) localization (D–F) in cells of the apical meristem. In mature cortical cells (G–I), nuclear localization (arrowheads) is evident. Membrane association (arrows) is observed in both mature (G–I) and apical (J–L) cortical cells. The YFP-PP2AA3 fusion also exhibits ubiquitous accumulation in the root tip (M–O). Propidium iodide fluorescence (A, G, J, and M) and YFP fluorescence (B, D, H, K, and N) are overlaid (C, E, F, I, L, and O) in medial (A–F and M–O) and cortical (G–L) optical sections of 4-dpg roots of lines *rcn1* RYR-80 (A–L) and *rcn1* AYA-2 (M–O). Beam intensity was increased for imaging YFP fluorescence in line *rcn1* AYA-2 (N and O; compare with Supplemental Fig. S4, E and F). Scale bars, 25 $\mu$m (A–C and G–O) and 10 $\mu$m (D–F).

altered AGL42-GFP expression in auxin-treated root tips (data not shown). Furthermore, publicly available microarray data indicate that *AGL42* expression changes less than 1.5-fold in response to indole-3-acetic acid or naphthylacetic acid treatment (AtGenExpress Hormone Response and Genvestigator Stimulus data sets).

We asked whether the activity of an auxin-responsive reporter construct was altered in the *rcn1* mutant. As described previously (Sabatini et al., 1999), wild-type seedlings carrying the *DR5-GUS* reporter show most intense staining around the columella initials, with lower GUS activity levels in the QC and throughout the columella (Fig. 4I). In *rcn1 DR5-GUS* roots, the overall intensity of staining was reduced, and *rcn1* roots frequently exhibited more intense staining in the external columella layer than in the region around the columella initials (Fig. 4J). Similar results were obtained with wild-type and *rcn1 DR5-GUS* lines backcrossed twice into the Ws genetic background (Fig. 4, K and L). Cantharidin-treated wild-type *DR5-GUS* seedlings also showed a reduction in staining intensity, as was reported previously (Shin et al., 2005; data not shown). Reduced activity of a DR5rev reporter was recently reported for seedlings carrying a *pp2aa2* or *pp2aa3* mutation in combination with *rcn1* (Michniewicz et al., 2007). Our results indicate that even modest reductions in phosphatase activity reduce auxin concentrations around the initial cells and compromise meristem function. The ability of cantharidin treatment to mimic *rcn1* defects suggests that auxin distribution and QC identity are regulated by postembryonic *RCN1* function.

### Abundance and Localization of YFP Fusion Proteins

We assayed the levels of transgene expression in roots via immunoblotting with anti-RCN1 and anti-GFP antibodies (Supplemental Fig. S3). Anti-RCN1 immunoblots show that accumulation of the fusion proteins in the *RYR* and *RRY* lines was comparable to that of native RCN1 protein in wild-type plants. Use of anti-GFP antibodies allowed direct comparison of fusion protein abundance, which was similar in *RYA*, *RYR*, and *RRY* lines, and somewhat greater than in *AYA* lines. These results show that intact fusion protein accumulates at levels comparable to those of the endogenous A subunits and indicate that complementation of the *rcn1* defects by *YFP-RCN1* does not require gross overexpression of the fusion protein.

We also assayed the expression and subcellular localization of the YFP fusions using confocal microscopy. In a recent study, immunolocalization of an RCN1-YFP fusion in cells of the root apex detected cytoplasmic, perinuclear, and peripheral localization (Michniewicz et al., 2007). Consistent with this result, we observed that both RCN1-YFP fusion proteins were abundant and ubiquitous in root tips, with cytoplasmic and strong perinuclear signal accumulating in all cell types at the root apex (Fig. 5, A–F). Interestingly, although cells in the region of the root apical meristem (and distal elongation zone) exhibited very little nuclear RCN1-YFP signal, vacuolated cells in more mature regions of the root exhibited nuclear as well as cytoplasmic accumulation (Fig. 5, D–F versus G–I). Optical sectioning confirmed that the fusion protein was present inside the nucleus of these cells (data not shown). Cells in the apical meristem and in more mature regions also exhibited strong peripheral signal, indicating enrichment around the plasma membrane; membrane enrichment was especially clear in cortical cells (Fig. 5, G–L; Supplemental Fig. S4, A–C). Strong accumulation of fusion protein also was observed in root hairs and lateral root primordia, with localization in lateral root primordia recapitulating that observed at the primary root tip (data not shown). Light- and dark-grown seedlings carrying the fusion constructs exhibited YFP fluorescence in roots and hypocotyls, with YFP accumulation patterns matching the previously reported RCN1 mRNA expression pattern (Deruère et al., 1999). Like vacuolated root cells, hypocotyl cells exhibited cytoplasmic, nuclear, and peripheral signal, with little or no accumulation evident in chloroplasts (data not shown).

To confirm that membrane localization was characteristic of the native forms of RCN1 and PP2AA3, we assayed the distribution of endogenous A subunits in soluble and microsomal membrane fractions isolated from wild-type seedlings (Fig. 6A). All three A subunits were abundant both in soluble and microsomal fractions, consistent with the analysis of YFP-RCN1 fusion protein localization. The catalytic subunit also was detected in microsomal fractions (data not shown). In contrast to PP2A subunits, the cytosolic PEPC protein was detected in soluble but not membrane fractions, indicating minimal contamination of the membrane fraction with cytoplasmic proteins. We detected PP2AA2 and PP2AA3 in membranes extracted from *rcn1*

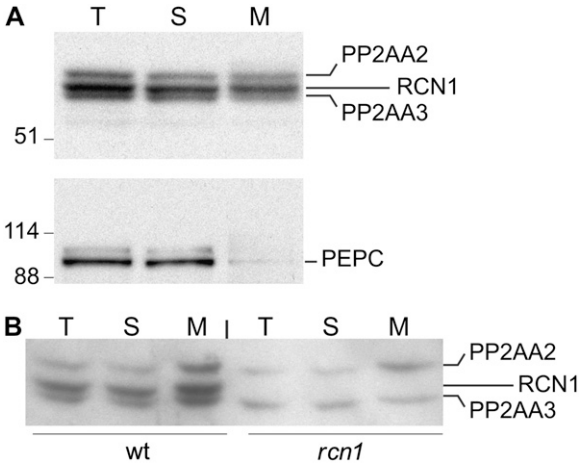


**Figure 6.** Subcellular fractionation of native A subunit isoforms. Soluble and microsomal membrane fractions were prepared from whole wild-type seedlings (A) or roots of wild-type and *rcn1* plants (B), and subjected to SDS-PAGE and immunoblotting analysis using anti-RCN1 (top) and anti-PEPC (bottom) antibodies. T, Total; S, soluble; M, microsomal membrane.

mutant roots, and all three isoforms in the membrane fraction from wild-type roots (Fig. 6B). These data indicate that PP2A complexes associate with membranes in growing seedlings. The presence of all three A subunit proteins in the microsomal fraction indicates that membrane association is not an isoform-specific characteristic. It is possible that recruitment of PP2A to a cellular membrane may allow it to interact with substrate or regulator proteins on the same membrane. Although the primary amino acid sequences of the A and C subunits do not contain motifs that predict membrane localization, several recent studies have shown that PP2A may interact with plasma membrane components, including the plasma membrane $H^+$-ATPase and the signaling lipid phosphatidic acid (Michniewicz et al., 2007).

Subcellular localization of the YFP-PP2AA3 fusion protein was similar to that of YFP-RCN1. Under control of the *RCN1* promoter, accumulation of the YFP-PP2AA3 fusion was similar to that of YFP-RCN1 (see Supplemental Fig. S4D). Expression of YFP-PP2AA3 under control of the *PP2AA3* regulatory region resulted in decreased abundance of the fusion protein, with the strongest accumulation evident in the vascular cylinder (Fig. 5, M–O; Supplemental Fig. S4, E and F). At this lower abundance, subcellular localization patterns were difficult to assess, but perinuclear, cytoplasmic, and peripheral localization were detected in most roots. These results suggest that RCN1 is more abundant than PP2AA3 in wild-type roots.

### RCN1 Performs an Isoform-Specific Function in Root Stress Response

Given the unique role of *RCN1* in regulating root growth and the stress sensitivity of PP2A mutants in

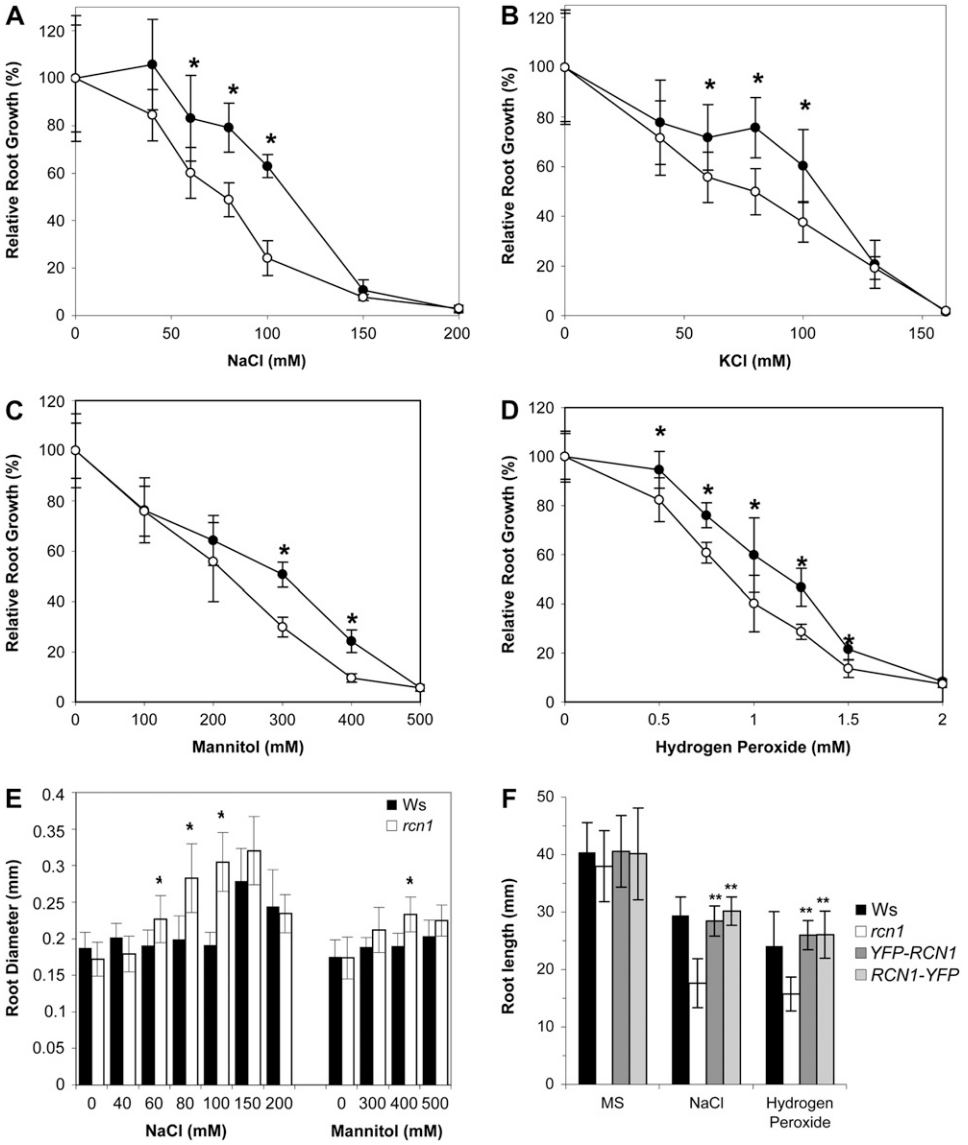


**Figure 7.** Stress sensitivity is increased in *rcn1* seedlings. Wild-type (black symbols) and *rcn1-1* mutant seedlings (white symbols) were transferred from standard medium to plates containing the indicated concentrations of NaCl (A), KCl (B), mannitol (C), and hydrogen peroxide (D). New growth (elongation from the point of transfer) was measured after 7 d of additional growth. E, Root diameter at the midpoint of the new growth segment was measured for plants grown on NaCl and mannitol. F, Overall root length was measured on wild-type, mutant, and complemented mutant seedlings (transgenic lines R1H9 and R2Q3; see "Materials and Methods") transferred to NaCl- or hydrogen peroxide-containing plates as described above. For all panels, each value shown represents the average for 12 to 15 seedlings; error bars indicate SD. Asterisks indicate levels of statistical significance as determined by Student's *t* test: *, $P < 0.002$ for *rcn1* versus wild type; **, $P < 10^{-7}$ versus *rcn1* and $P > 0.2$ versus Ws.

yeast, we asked whether *rcn1* mutant plants show stress sensitivity similar to that observed in *tpd3* yeast cells. Roots of mutant seedlings exhibited increased sensitivity to ionic ($Na^+$, $K^+$), osmotic (mannitol), and oxidative (hydrogen peroxide) stress with decreased elongation across a range of concentrations (Fig. 7, A–D). Sodium and mannitol treatment also caused radial expansion, which was enhanced in the cortical cell layer of *rcn1* roots (Fig. 7E; Supplemental Fig. S5). Oxidative stress inhibited elongation (Fig. 7D) but did not cause radial swelling of wild-type or mutant roots (data not shown). Both *YFP-RCN1* and *RCN1-YFP* fusion transgenes restored wild-type stress tolerance to *rcn1* mutant roots (Fig. 7F). These data indicate that RCN1 regulation of PP2A activity is required for normal stress tolerance in seedling roots. We did not detect differences in salt sensitivities of adult wild-type and *rcn1* plants, suggesting that the stress sensitivity of *rcn1* is limited to the seedling stage (data not shown).

Unlike *rcn1*, the *pp2aa2* and *pp2aa3* single mutants and the *pp2aa2 pp2aa3* double mutant exhibited stress sensitivities that very nearly matched that of the parental wild type (see Supplemental Fig. S6). Despite the presence of PP2AA2 and PP2AA3 proteins in root tissue (Zhou et al., 2004), these regulatory A subunit isoforms do not appear to play an equivalent role in stress tolerance. We asked whether the amino acid sequences for RCN1, PP2AA2, and PP2AA3 exhibit discrete differences that might confer biological specificity. The predicted RCN1 protein shares 86% identity with both PP2AA2 and PP2AA3 (see Supplemental Fig. S1A; Slabas et al., 1994), and most of the strongly conserved residues defined in mammalian A subunits are conserved in all three Arabidopsis isoforms. However, Tyr-450, one putative component of the hydrophobic interaction interface (Ruediger et al., 1994; Groves et al., 1999; Xing et al., 2006), is replaced by a basic residue (His) in PP2AA2 and PP2AA3 (see Supplemental Fig. S1A). Mutagenesis of the *RCN1-YFP* fusion to generate a His-450 allele does not compromise complementation of temperature, sorbitol, and sodium chloride sensitivity of *tpd3* yeast cells (data not shown), suggesting that Tyr-450 does not play a required role in mediating stress tolerance. Intriguingly, database searches suggest that the His-450 A subunit may be a plant-specific variant. A Tyr residue is conserved at this position in A subunits of all vertebrates and insects, in yeast, and in many plant species (pea [*Pisum sativum*], tobacco [*Nicotiana tabacum*], *Brassica* spp., *Medicago* spp., and *Lolium* spp.). Rice, maize, several other grasses, many fungi, and *Caenorhabditis elegans* carry Phe at this position. His-450 isoforms are found only in plant genomes that also encode a Tyr-450 isoform (e.g. those of *Vicia*, *Medicago*, *Brassica*, and Arabidopsis) and in *Thellungiella salsuginea*, for which limited sequence data are available. The His-450 variant thus appears to be a plant-specific regulatory A subunit isoform, and may occur only in plants that also encode a Tyr-450 isoform.

## DISCUSSION

Our analysis of Arabidopsis A subunit functions in vivo demonstrates unique functions for *RCN1* in specific cell types in seedlings. The requirement for *RCN1* function in maintaining normal root stem cell organization is not explained by cell- or tissue-specific mRNA expression patterns because expression of *PP2AA3* under control of the *RCN1* promoter does not fully rescue normal cell division patterns. In hypocotyl tissue, rescue of normal cell expansion by *PP2AA3* expression demonstrates overlapping function of the A subunit isoforms. Our data support the hypothesis that root growth and stress response are regulated by PP2A substrates specifically targeted by RCN1, whereas targeting of substrates involved in hypocotyl growth is not dependent on a particular A subunit isoform. Organization and function of stem cells at the root apex, as measured by formation of normal columella tiers and expression of a marker for QC identity, is compromised by reduced PP2A function during postembryonic development. Given that the subcellular localization of RCN1 and PP2AA3 proteins appears similar, functional specificity is likely to depend on isoform-specific protein-protein interactions with substrates or regulators of the complex.

### Dosage Sensitivity versus Isoform Specificity in A Subunit Function

*YFP-PP2AA3* fusion constructs that provide only weak complementation of the *rcn1* root tip phenotype robustly rescue hypocotyl elongation. These findings suggest that hypocotyl elongation requires a threshold level of A subunit function, with no stringent requirement for RCN1-specific amino acid sequences. Even a modest level of YFP-PP2AA3 expression in the *rcn1* mutant is sufficient to promote normal hypocotyl elongation. Because increased ethylene synthesis in dark-grown *rcn1* seedlings contributes significantly to reduced hypocotyl growth (Larsen and Chang, 2001; Muday et al., 2006), this result suggests that PP2A complexes containing the PP2AA3 isoform are competent for down-regulation of ethylene biosynthesis. In contrast, *PP2AA3* rescues root tip organization weakly even when expression is driven by the *RCN1* promoter, demonstrating a more stringent requirement for A subunit function in the root apical meristem. Although it is possible that high-level overexpression of PP2AA3 could suppress this stem cell defect, our data clearly indicate that RCN1-containing PP2A complexes effectively target the key substrates for root growth at physiological expression levels, whereas PP2AA3-containing complexes do not.

RCN1 may be the preferred interaction partner for C and B subunits most active in seedling roots. The A$\alpha$ and A$\beta$ isoforms of mammalian PP2A differ in their binding activities (Zhou et al., 2003; Sablina et al., 2007). However, the positive regulatory effect of RCN1 also is consistent with the hypothesis that RCN1 plays

a role in an activation cycle for Arabidopsis C subunits analogous to that of TPD3 in yeast, promoting interaction with PTPA/RRD (Hombauer et al., 2007). The modest effects of loss of PP2AA2 and PP2AA3 function could indicate that these scaffolds do not interact efficiently with PTPA/RRD-like activators, and therefore do not have equivalent effects on overall PP2A activity, at least in the presence of functional RCN1.

### RCN1 Plays an Isoform-Specific Role in Root Development

Our data provide new insight into the developmental effects of increased phosphorylation of RCN1-specific PP2A substrates, demonstrating that loss of RCN1 regulation alters stem cell function and auxin distribution without producing the meristem collapse phenotype caused by more drastic reductions in PP2A activity. Previous studies have documented ectopic expression of cell identity markers and abnormal cell division patterns caused by treatment with exogenous auxin or loss of auxin transporter function in shoots and roots (Sabatini et al., 1999; Benkova et al., 2003; Blilou et al., 2005). Our results indicate that meristem function is also sensitive to subtle changes in auxin flux, as well as to those more profound ones. Moreover, inhibition of phosphatase function during the seedling phase alone is sufficient to perturb meristem function, showing that root tip patterning is a dynamic process that responds rapidly to altered phosphorylation levels.

*RCN1* plays a key role in maintaining the patterns of root meristem cell division and function. Decreased expression of the *DR5-GUS* reporter in *rcn1* roots and of the QC marker *AGL42-GFP* in cantharidin-treated roots suggests that normal establishment of the local auxin concentration maximum and full expression of QC identity require RCN1-regulated PP2A activity. Because positioning of a local maximum in the auxin pool at the root apex is an important patterning determinant (Sabatini et al., 1999), increased basipetal auxin transport in *rcn1* could affect root tip organization by altering the position of the auxin concentration maximum or by more generally increasing flux through the auxin transport stream in the root tip. Consistent with this hypothesis, the strongly reduced expression of DR5rev-GFP that is observed in *rcn1 pp2aa3* and *rcn1 pp2aa2/+* root tips is rescued by 1-*N*-naphthylphthalamic acid treatment (Michniewicz et al., 2007).

Previous studies have revealed complex feedback loops connecting ethylene response with auxin homeostasis in roots (Stepanova et al., 2005; Chilley et al., 2006). Furthermore, increased ethylene response was recently shown to stimulate cell divisions in the QC (Ortega-Martinez et al., 2007). Two observations argue against the hypothesis that increased ethylene response accounts for aberrant QC function in *rcn1*. First, we observe altered root tip morphology in light-grown seedlings, whereas increased ethylene synthesis was observed only in dark-grown *rcn1* seedlings (Muday et al., 2006). Second, although *rcn1* may enhance ethylene sensitivity in shoots (Larsen and Chang, 2001), *ctr1* root phenotypes are suppressed in the *rcn1 ctr1* double mutant (Larsen and Chang, 2001; A. DeLong, unpublished data), suggesting that loss of *rcn1* reduces ethylene response in roots. Interestingly, ethylene treatment stimulates auxin accumulation in wild-type root tips, and mutations that reduce ethylene-induced auxin production confer weak ethylene insensitivity (Stepanova et al., 2005). Thus increased basipetal auxin transport also may result in decreased sensitivity to ethylene in *rcn1* roots.

### Subcellular Localization of RCN1 and A3 Proteins

Our data suggest that nuclear localization of RCN1 is developmentally regulated in roots. YFP-RCN1 was abundant in perinuclear and cytoplasmic compartments, but was underrepresented in nuclei of meristematic and central elongation zone cells (Fig. 5). Nuclear localization was observed in more mature cells in and above the proximal elongation zone, with little or no perinuclear accumulation evident in these cells. These data are consistent with the idea that RCN1 localization is dynamic during root cell differentiation, with enrichment in the perinuclear compartment in rapidly dividing cells and nuclear enrichment in postmitotic cells. Interestingly, a GFP fusion to the OXIDATIVE SIGNAL-INDUCIBLE1 (OXI1) protein kinase, a member of the AGC kinase family that also includes the PINOID kinase, suggests that subcellular localization of OXI1 in root hairs also may be developmentally regulated, with nuclear accumulation occurring late in root hair development (Anthony et al., 2004; Rentel et al., 2004). Like RCN1, OXI1 plays a role in oxidative stress response; OXI1 activity increases under oxidative stress conditions, and promotes pathogen resistance and root hair development. Developmentally regulated localization of kinase/phosphatase pairs would provide an additional level of fine-tuning in phosphorylation-based control circuits.

We also observed peripheral localization of YFP-RCN1 and YFP-PP2AA3 in all cell types in the root tip. Membrane association appeared fairly uniform around the cell periphery, and did not exhibit obvious polarity or asymmetry in these experiments. Our cell fractionation data are consistent with the existence of a significant pool of membrane-associated PP2A in seedlings. Membrane association of PP2A complexes has been reported in several contexts previously, including early mouse development, during tight junction formation, and during associations with endothelial nitric oxide synthase at the plasma membrane (Gotz et al., 2000; Nunbhakdi-Craig et al., 2002; Wei and Xia, 2006). Arabidopsis PP2A interacts with the C terminus of the plasma membrane ATPase AHA2 in vitro and exhibits partial colocalization with the PIN1 and PIN2 proteins in roots (Fuglsang et al., 2006; Michniewicz et al., 2007). Additionally, RCN1 protein binds phosphatidic acid,

a lipid signaling molecule that recruits target proteins to the plasma membrane and plays a significant role in abiotic stress response (Meijer and Munnik, 2003; Testerink et al., 2004). Recruitment of PP2A to a membrane compartment via phosphatidic acid binding could alter phosphatase activity toward membrane-associated substrates. Membrane-associated PP2A activity may be critical for regulation of auxin transport, stress response, and regulation of stem cell function in roots.

### Stress Sensitivity in *rcn1* Seedlings

The data presented here indicate that *RCN1* function plays a unique role in mediating root stress response. Our working model states that positive regulation of PP2A activity by the RCN1 protein contributes to a response that maintains normal growth under a wide range of stress conditions. As a modulator of auxin, ethylene, and ABA levels and/or responses, *RCN1* is well positioned to act as an integrator of stress signaling. Abiotic stress may alter the cellular localization and amount of PP2A activity, resulting in PP2A-induced alterations in hormone responses. Loss of *RCN1* function compromises these adaptive alterations in PP2A localization and/or activity, leading to increased growth inhibition under stress conditions.

Previous studies focusing on two PP2A interactors, TAP46 and the AtCHIP E3 ubiquitin ligase, suggested that PP2A may play a role in the chilling response in Arabidopsis (Harris et al., 1999; Luo et al., 2006). Additionally, gene expression studies show that mRNAs for PP2A catalytic subunits in rice are differentially expressed in response to drought, salinity, and heat stress (Yu et al., 2003). An Arabidopsis PP2A catalytic subunit mutant was recently found to affect ABA-related stress responses through negative regulation of ABA signaling. Although loss of *PP2AC-2* function confers ABA hypersensitivity (Pernas et al., 2007), loss of *RCN1* function results in reduced ABA sensitivity (Kwak et al., 2002). Paradoxically, both mutants show increased sensitivity to NaCl treatment. However, the *pp2ac-2* mutant exhibits a sensitivity phenotype specific for ABA-related stress (Pernas et al., 2007) unlike the general stress sensitivity phenotype reported here for *rcn1*. These disparities indicate that the effect of *rcn1* loss of function is unlikely to be mediated by a specific effect on regulation of PP2AC-2 activity.

The parallel stress sensitivity of *rcn1* plants and *tpd3* yeast is striking, but it is not clear that the mechanism involved in the plant and yeast stress responses is similar. Interestingly, the transition between perinuclear enrichment and intranuclear YFP-RCN1 localization occurs in cells of the elongation zone, the same cell population that would be responsible for altered elongation under stress conditions. In yeast, PP2A is required for nuclear accumulation of the stress-responsive transcription factor Msn2p after nutrient deprivation, rapamycin treatment, and temperature and ionic stress (Santhanam et al., 2004). Regulation by PP2A has been proposed to involve dephosphorylation of a nuclear export signal in Msn2p. Although we cannot rule out a similar explanation for the stress sensitivity of *rcn1* seedlings, there are no obvious orthologs of the Msn2 and Msn4 transcription factors in the Arabidopsis genome (A. DeLong, unpublished data). The Arabidopsis C2H2 zinc finger proteins that produce the best BLAST scores against Msn2 and Msn4 are more closely related to the TFIIIA family of transcription factors than to Msn2p or Msn4p. Additionally, we assayed for but did not observe an enhancement of nuclear RCN1 localization under stress conditions (see Supplemental Fig. S7). Over a range of salt treatment times from minutes to 18 h we did not detect any alteration in the nuclear versus perinuclear YFP-RCN1 localization pattern, though some experiments suggested enrichment of the membrane-associated population after short-term salt treatment (J.J. Blakeslee and A. DeLong, unpublished data). Additional biochemical experiments will be required to explore this possible membrane recruitment more rigorously.

## MATERIALS AND METHODS

### Plant Material and Growth Conditions

The *rcn1-1* allele (Garbers et al., 1996) and derived transgenic lines (see below) were compared with the parental Ws line. An *rcn1-1* line homozygous for the *DR5-GUS* reporter (Rashotte et al., 2001) was backcrossed twice to the parental *DR5-GUS* line (Col background) or to *rcn1-1* and Ws to introgress the *rcn1-1* mutation or the reporter, respectively, into a more uniform genetic background. Plants homozygous for the *rcn1-1* mutation were identified among the self-progeny of the *DR5-GUS* backcross products; homozygosity of the *DR5-GUS* marker was confirmed in self-progeny of these *rcn1* individuals. A similar procedure was used to isolate families homozygous for the DR5 reporter from the *rcn1-1* backcross. The *rcn1-6* allele is the T-DNA insertion allele SALK_059903 (kind gift of X. Wang and J. Chory, Salk Institute) and is compared with the parental Col-0 line. *AGL42-GFP* (Nawy et al., 2005) was the kind gift of B. Kelley and P. Benfey (Duke University).

Plants were grown as described previously (Zhou et al., 2004). For stress sensitivity measurements, seedlings were grown on vertical plates for 4 d in constant light at 24°C on standard medium (0.5× Murashige and Skoog salts containing 1% Suc and 1% agar), then transferred to the same medium supplemented with the indicated salt, mannitol, and hydrogen peroxide concentrations. Root tips of five mutant and five wild-type seedlings were aligned at a marked position on each plate and plates were returned to constant light. New growth was measured 7 d later using National Institutes of Health ImageJ software, and relative new root growth was calculated as a percentage of that obtained on fresh standard medium. Each data point represents the average for 15 seedlings. Hypocotyl elongation assays were performed as described previously (Deruère et al., 1999; Zhou et al., 2004). After scanning each plate to allow measurement of hypocotyl lengths, each seedling was scored for YFP fluorescence using a Leica MZFLIII dissecting microscope equipped with a mercury arc lamp and a GFP filter set.

### Construction of YFP Fusions

The *ADC1*$_{pro}$*:RCN1-YFP* fusions for yeast were constructed using the TT-PCR strategy (Tian et al., 2004), with the *RCN1* cDNA (Garbers et al., 1996), the *ADC1* alcohol dehydrogenase promoter of pAAH5 (Ammerer, 1983), and pYFP3 (kind gift of D. Jackson, Cold Spring Harbor Laboratory) as templates for the partial PCR products. PCR primer sequences are given in Supplemental Table S1. The *ADC1*$_{pro}$*:RCN1-YFP* fusions were obtained and cloned into YEplac195 (Pitluk et al., 1995) using the Gateway and TOPO-XL systems (Invitrogen). The genomic *RCN1-YFP* and *YFP-RCN1* fusions for plant transformation also were constructed via TT-PCR using pYFP3 and wild-type

Col-0 genomic DNA. To simplify cloning, the original TT-PCR products contained a short promoter region (861 bp total upstream from the *RCN1* ATG). The resulting fusion was cloned into pPZP221 (Hajdukiewicz et al., 1994) using the Gateway system (Invitrogen). The insert was sequenced and coding errors were corrected by QuikChange II XL site-directed mutagenesis (Stratagene). A longer promoter fragment containing 2.1 kb of genomic sequence upstream from the start of the RCN1 transcript was amplified from Col-0 genomic DNA and substituted for the short promoter in the binary vector, yielding $RCN_{pro}$:*YFP-RCN* (*RYR*). To generate the $RCN_{pro}$:*YFP-PP2AA3* (*RYA*) fusion, the *PP2AA3* coding sequence was amplified from RAFL09-82-A21 (RIKEN BRC) and substituted for the *RCN1* coding region in *RYR*. For $PP2AA3_{pro}$:*YFP-PP2AA3* (*AYA*), a 1.2-kb *PP2AA3* promoter fragment was amplified from Col-0 genomic DNA and substituted for the *RCN1* promoter region in $RCN_{pro}$:*YFP-PP2AA3*. For $PP2AA3_{pro}$:*PP2AA3* the *YFP* coding sequence was deleted by oligonucleotide-mediated mutagenesis. All constructs were sequence verified and coding sequence errors were corrected by oligonucleotide-mediated mutagenesis. All clones were electroporated into *Agrobacterium tumefaciens* strain GV3101 for transformation into *rcn1-1* plants via floral dip (Bechtold et al., 1993; Garbers et al., 1996). All transformants were selected for gentamycin resistance. T-DNA copy numbers were determined by screening gentamycin resistance segregation ratios followed by Southern-blot analysis using a probe for the pPZP221 gentamycin resistance gene. The RYR-80, RYR-85, RYR-86, RRY-90, RRY-92, RYA-28, RYA-33, and AYA-2 lines carry single-copy T-DNAs, whereas the RYR-66, RYR-74, RYA-32, and AYA-6 lines carry two T-DNA copies and AYA-16 and AYA-100 carry three or more copies. The R2Q3 line carries three or more copies of the *RCN1-YFP* fusion driven by the short *RCN1* promoter fragment described above.

## Microscopy and Detection of Reporter Gene Expression

For confocal imaging, seedlings were grown in constant light at 20°C on standard medium, stained lightly with propidium iodide (10 $\mu$g mL$^{-1}$) or FM4-64 (5 $\mu$g mL$^{-1}$), and mounted immediately for confocal analysis. For seedlings grown on NaCl, osmotic and ionic concentrations were maintained throughout the staining and mounting process. YFP fusion protein localization and seedling root tip morphology were examined by confocal microscopy using a Leica TCS SP2 AOBS spectral confocal microscope. To image YFP fusion proteins and root tip architecture, YFP fluorescence was excited at 514 nm and collected at 525 to 560 nm and propidium iodide fluorescence was excited at 593 nm and collected at 610 to 680 nm using a pinhole of 1 a.u. To image *AGL42-GFP*, GFP fluorescence was excited at 488 nm and collected at 495 to 550 nm and FM4-64 fluorescence was excited at 593 nm and collected at 650 to 800 nm with a pinhole setting of 2 a.u. and using sequential scanning. Images were processed using Leica confocal software (LCS Lite). To maintain comparable fluorescence signals, images were collected using constant beam intensities and settings within each experiment, unless otherwise noted. For starch staining, 4-dpg seedlings were cleared and stained with iodine-potassium iodide (Fukaki et al., 1998) before imaging on a Zeiss Axiovert 200M. To detect *DR5-GUS* expression, seedlings were gently vacuum infiltrated and then stained overnight in 100 mM sodium phosphatase, pH 7.0, 10 mM EDTA, 0.5 mM potassium ferricyanide, 0.5 mM potassium ferrocyanide, 0.1% Triton X-100, and 1 mM X-glucuronide, followed by clearing in 90% ethanol. Yeast cells were imaged using a Zeiss Axioplan 2 equipped with a 100× alphaPlan-FLUAR objective and Hamamatsu-ORCA camera (Hamamatsu Photonics), and images were collected with Openlabs software (Improvision).

## Yeast Complementation Assays

Yeast strain Y1459 (*tpd3-1*; van Zyl et al., 1992) was transformed with YEpTPD3 (kind gift of J. Broach, Princeton University), YEplac195, $ADH_{pro}$:RCN1, $ADH_{pro}$:YFP-RCN1, $ADH_{pro}$:RCN1-YFP, and $ADH_{pro}$:$RCN1_{Y450H}$-YFP using a standard lithium acetate transformation protocol (Ausubel et al., 1992). For serial dilution assays, cultures were grown in yeast peptone dextrose (YPD) liquid medium at 30°C, diluted to an $OD_{600}$ of 2, then diluted in 10-fold steps into fresh YPD. Ten microliters of each dilution was spotted onto YPD medium or YPD supplemented with 600 mM NaCl. The SUP35:GFP strain (Satpute-Krishnan and Serio, 2005) was the kind gift of T. Serio (Brown University).

## Preparation of Microsomal Membranes

Microsomal membrane fractions were prepared as described (Blakeslee et al., 2007), with the following modifications. Dark-grown whole seedlings or roots were harvested at 5 dpg, ground, and microsomal membranes were isolated by spinning at 100,000*g* for 1 h. Membrane fractions were washed twice, flash-frozen, and stored at −80°C. For immunoblot analysis, membrane fractions were solubilized with 1% Triton X-100.

## Immunoblot Analysis

For immunoblot analysis, yeast cells were grown to log phase in YPD at 30°C, harvested by centrifugation, resuspended on ice in 100 mM Tris, pH 7.5, 100 mM EDTA, 5 mM dithiothreitol, 2 mM phenylmethylsulfonyl fluoride, 5 $\mu$g/mL pepstatin, and 100 $\mu$g/mL aprotinin and leupeptin, and lysed by vortexing with glass beads. The resulting extracts were cleared by low-speed centrifugation and immediately boiled with Laemmli buffer. Plant extract preparation, SDS-PAGE, and immunoblotting techniques were as described previously (Deruère et al., 1999), except that immunoblots were treated with 0.2 M NaOH at 37°C for 20 min immediately after transfer, followed by five PBST washes before blocking. Antisera used were anti-GFP (JL-8; CLONTECH), anti-PEP carboxylase (Rockland), anti-RCN1 (Deruère et al., 1999), and anti-C antibodies raised against the C-terminal peptide (CEPDTTRKTPDYFL) of Arabidopsis (*Arabidopsis thaliana*) PP2A-C1.

The Arabidopsis Genome Initiative locus identifiers for genes described in this article are as follows: *RCN1* (also known as *RegA*, *EER1*, and *PP2AA1*; At1g25490), *PP2AA3* (also known as *PDF2*; At1g13320), *PP2AA2* (also known as *PDF1*; At3g25800), and *AGL42* (At5g62165).

## Supplemental Data

The following materials are available in the online version of this article.

**Supplemental Figure S1.** Structural model of sequence differences between Arabidopsis A subunit isoforms.

**Supplemental Figure S2.** *RCN1* is haploinsufficient in the *pp2aa2 pp2aa3* background.

**Supplemental Figure S3.** Regulatory A subunit transgene products accumulate to native levels.

**Supplemental Figure S4.** Accumulation and localization of YFP-PP2AA3 fusion proteins.

**Supplemental Figure S5.** Expansion of cortical cells in salt-stressed *rcn1* seedlings.

**Supplemental Figure S6.** Normal stress sensitivity in *pp2aa2* and *pp2aa3* mutants.

**Supplemental Figure S7.** Localization of a YFP-RCN1 fusion protein after NaCl treatment.

**Supplemental Table S1.** PCR primers.

## ACKNOWLEDGMENTS

We gratefully acknowledge D. Jackson for TT-PCR reagents and advice, T. Serio for advice on yeast culture and imaging, A. Dunaevsky for FM4-64, and P. Benfey and T. Nawy for seed stocks and advice on QC markers. We thank J. Bender, M. Johnson, G. Muday, and F. Tax for critical reading of the manuscript and for helpful discussions. We thank G. Williams, R. Creton, and J. Nathanson for expert advice on imaging. We thank M. Clarke-Pearson, T. Simolari, R. Luo, and S. Cho for assistance with transgenic plant lines, and F. Jackson and B. Leib for greenhouse care.

Received November 9, 2007; accepted December 17, 2007; published December 27, 2007.

## LITERATURE CITED

**Ammerer G** (1983) Expression of genes in yeast using the *ADC1* promoter. Methods Enzymol **101:** 192–201

**Andrade MA, Bork P** (1995) HEAT repeats in the Huntington's disease protein. Nat Genet **11:** 115–116

**Anthony RG, Henriques R, Helfer A, Meszaros T, Rios G, Testerink C, Munnik T, Deak M, Koncz C, Bogre L** (2004) A protein kinase target of a

PDK1 signalling pathway is involved in root hair growth in Arabidopsis. EMBO J **23:** 572–581

**Ausubel FM, Brent R, Kingston RE, Moore DD, Seidman JG, Smith JA, Struhl K** (1992) Current Protocols in Molecular Biology. Wiley-Interscience, New York

**Bechtold N, Ellis H, Pelletier G** (1993) *In planta Agrobacterium*-mediated gene transfer by infiltration of adult *Arabidopsis thaliana* plants. C R Acad Sci Ser III Sci Vie **316:** 1194–1199

**Benfey PN, Scheres B** (2000) Root development. Curr Biol **10:** R813–R815

**Benkova E, Michniewicz M, Sauer M, Teichmann T, Seifertova D, Jurgens G, Friml J** (2003) Local, efflux-dependent auxin gradients as a common module for plant organ formation. Cell **115:** 591–602

**Blakeslee JJ, Bandyopadhyay A, Lee OR, Mravec J, Titapiwatanakun B, Sauer M, Makam SN, Cheng Y, Bouchard R, Adamec J, et al** (2007) Interactions among PIN-FORMED and P-glycoprotein auxin transporters in *Arabidopsis.* Plant Cell **19:** 131–147

**Blilou I, Xu J, Wildwater M, Willemsen V, Paponov I, Friml J, Heidstra R, Aida M, Palme K, Scheres B** (2005) The PIN auxin efflux facilitator network controls growth and patterning in Arabidopsis roots. Nature **433:** 39–44

**Camilleri C, Azimzadeh J, Pastuglia M, Bellini C, Grandjean O, Bouchez D** (2002) The *Arabidopsis TONNEAU2* gene encodes a putative novel protein phosphatase 2A regulatory subunit essential for the control of the cortical cytoskeleton. Plant Cell **14:** 833–845

**Chilley PM, Casson SA, Tarkowski P, Hawkins N, Wang KL, Hussey PJ, Beale M, Ecker JR, Sandberg GK, Lindsey K** (2006) The POLARIS peptide of *Arabidopsis* regulates auxin transport and root growth via effects on ethylene signaling. Plant Cell **18:** 3058–3072

**DeLong A** (2006) Switching the flip: protein phosphatase roles in signaling pathways. Curr Opin Plant Biol **9:** 470–477

**Deruère J, Jackson K, Garbers C, Söll D, DeLong A** (1999) The *RCN1*-encoded A subunit of protein phosphatase 2A increases phosphatase activity in vivo. Plant J **20:** 389–399

**Fuglsang AT, Tulinius G, Cui N, Palmgren MG** (2006) Protein phosphatase 2A scaffolding subunit A interacts with plasma membrane H+-ATPase C-terminus in the same region as 14-3-3 protein. Physiol Plant **128:** 334–340

**Fukaki H, Wysocka-Diller J, Kato T, Fujisawa H, Benfey PN, Tasaka M** (1998) Genetic evidence that the endodermis is essential for shoot gravitropism in *Arabidopsis thaliana.* Plant J **14:** 425–430

**Garbers C, DeLong A, Deruère J, Bernasconi P, Söll D** (1996) A mutation in protein phosphatase 2A regulatory subunit A affects auxin transport in Arabidopsis. EMBO J **15:** 2115–2124

**Gotz J, Probst A, Mistl C, Nitsch RM, Ehler E** (2000) Distinct role of protein phosphatase 2A subunit Calpha in the regulation of E-cadherin and beta-catenin during development. Mech Dev **93:** 83–93

**Groves MR, Hanlon N, Turowski P, Hemmings BA, Barford D** (1999) The structure of the protein phosphatase 2A PR65/A subunit reveals the conformation of its 15 tandemly repeated HEAT motifs. Cell **96:** 99–110

**Hajdukiewicz P, Svab Z, Maliga P** (1994) The small, versatile pPZP family of Agrobacterium binary vectors for plant transformation. Plant Mol Biol **25:** 989–994

**Harris DM, Myrick TL, Rundle SJ** (1999) The Arabidopsis homolog of yeast TAP42 and mammalian alpha4 binds to the catalytic subunit of protein phosphatase 2A and is induced by chilling. Plant Physiol **121:** 609–617

**Hombauer H, Weismann D, Mudrak I, Stanzel C, Fellner T, Lackner DH, Ogris E** (2007) Generation of active protein phosphatase 2A is coupled to holoenzyme assembly. PLoS Biol **5:** e155

**Janssens V, Goris J** (2001) Protein phosphatase 2A: a highly regulated family of serine/threonine phosphatases implicated in cell growth and signalling. Biochem J **353:** 417–439

**Kerk D, Conley TR, Rodriguez FA, Tran HT, Nimick M, Muench DG, Moorhead GB** (2006) A chloroplast-localized dual-specificity protein phosphatase in Arabidopsis contains a phylogenetically dispersed and ancient carbohydrate-binding domain, which binds the polysaccharide starch. Plant J **46:** 400–413

**Kinoshita K, Nemoto T, Nabeshima K, Kondoh H, Niwa H, Yanagida M** (1996) The regulatory subunits of fission yeast protein phosphatase 2A (PP2A) affect cell morphogenesis, cell wall synthesis and cytokinesis. Genes Cells **1:** 29–45

**Kwak JM, Moon JH, Murata Y, Kuchitsu K, Leonhardt N, DeLong A, Schroeder JI** (2002) Disruption of a guard cell-expressed protein phosphatase 2A regulatory subunit, RCN1, confers abscisic acid insensitivity in *Arabidopsis.* Plant Cell **14:** 2849–2861

**Larsen PB, Cancel JD** (2003) Enhanced ethylene responsiveness in the Arabidopsis *eer1* mutant results from a loss-of-function mutation in the protein phosphatase 2A A regulatory subunit, *RCN1.* Plant J **34:** 709–718

**Larsen PB, Chang C** (2001) The Arabidopsis *eer1* mutant has enhanced ethylene responses in the hypocotyl and stem. Plant Physiol **125:** 1061–1073

**Lee JS, Ellis BE** (2007) Arabidopsis MAPK phosphatase 2 (MKP2) positively regulates oxidative stress tolerance and inactivates the MPK3 and MPK6 MAPKs. J Biol Chem **282:** 25020–25029

**Luo J, Shen G, Yan J, He C, Zhang H** (2006) AtCHIP functions as an E3 ubiquitin ligase of protein phosphatase 2A subunits and alters plant response to abscisic acid treatment. Plant J **46:** 649–657

**Meijer HJ, Munnik T** (2003) Phospholipid-based signaling in plants. Annu Rev Plant Biol **54:** 265–306

**Michniewicz M, Zago MK, Abas L, Weijers D, Schweighofer A, Meskiene I, Heisler MG, Ohno C, Zhang J, Huang F, et al** (2007) Antagonistic regulation of PIN phosphorylation by PP2A and PINOID directs auxin flux. Cell **130:** 1044–1056

**Muday GK, Brady SR, Argueso C, Deruere J, Kieber JJ, DeLong A** (2006) RCN1-regulated phosphatase activity and EIN2 modulate hypocotyl gravitropism by a mechanism that does not require ethylene signaling. Plant Physiol **141:** 1617–1629

**Nawy T, Lee JY, Colinas J, Wang JY, Thongrod SC, Malamy JE, Birnbaum K, Benfey PN** (2005) Transcriptional profile of the *Arabidopsis* root quiescent center. Plant Cell **17:** 1908–1925

**Niittyla T, Comparot-Moss S, Lue WL, Messerli G, Trevisan M, Seymour MD, Gatehouse JA, Villadsen D, Smith SM, Chen J, et al** (2006) Similar protein phosphatases control starch metabolism in plants and glycogen metabolism in mammals. J Biol Chem **281:** 11815–11818

**Nunbhakdi-Craig V, Machleidt T, Ogris E, Bellotto D, White CL III, Sontag E** (2002) Protein phosphatase 2A associates with and regulates atypical PKC and the epithelial tight junction complex. J Cell Biol **158:** 967–978

**Ortega-Martinez O, Pernas M, Carol RJ, Dolan L** (2007) Ethylene modulates stem cell division in the *Arabidopsis thaliana* root. Science **317:** 507–510

**Pernas M, Garcia-Casado G, Rojo E, Solano R, Sanchez-Serrano JJ** (2007) A protein phosphatase 2A catalytic subunit is a negative regulator of abscisic acid signalling. Plant J **51:** 763–778

**Pitluk ZW, McDonough M, Sangan P, Gonda DK** (1995) Novel CDC34 (UBC3) ubiquitin-conjugating enzyme mutants obtained by charge-to-alanine scanning mutagenesis. Mol Cell Biol **15:** 1210–1219

**Price NE, Mumby MC** (2000) Effects of regulatory subunits on the kinetics of protein phosphatase 2A. Biochemistry **39:** 11312–11318

**Rashotte AM, DeLong A, Muday GK** (2001) Genetic and chemical reductions in protein phosphatase activity alter auxin transport, gravity response, and lateral root growth. Plant Cell **13:** 1683–1697

**Rentel MC, Lecourieux D, Ouaked F, Usher SL, Petersen L, Okamoto H, Knight H, Peck SC, Grierson CS, Hirt H, et al** (2004) OXI1 kinase is necessary for oxidative burst-mediated signalling in Arabidopsis. Nature **427:** 858–861

**Ruediger R, Hentz M, Fait J, Mumby M, Walter G** (1994) Molecular model of the A subunit of protein phosphatase 2A: interaction with other subunits and tumor antigens. J Virol **68:** 123–129

**Sabatini S, Beis D, Wolkenfelt H, Murfett J, Guilfoyle T, Malamy J, Benfey P, Leyser O, Bechtold N, Weisbeek P, et al** (1999) An auxin-dependent distal organizer of pattern and polarity in the Arabidopsis root. Cell **99:** 463–472

**Sablina AA, Chen W, Arroyo JD, Corral L, Hector M, Bulmer SE, DeCaprio JA, Hahn WC** (2007) The tumor suppressor PP2A Abeta regulates the RalA GTPase. Cell **129:** 969–982

**Santhanam A, Hartley A, Duvel K, Broach JR, Garrett S** (2004) PP2A phosphatase activity is required for stress and Tor kinase regulation of yeast stress response factor Msn2p. Eukaryot Cell **3:** 1261–1271

**Satpute-Krishnan P, Serio TR** (2005) Prion protein remodelling confers an immediate phenotypic switch. Nature **437:** 262–265

**Schweighofer A, Hirt H, Meskiene I** (2004) Plant PP2C phosphatases: emerging functions in stress signaling. Trends Plant Sci **9:** 236–243

**Schweighofer A, Kazanaviciute V, Scheikl E, Teige M, Doczi R, Hirt H, Schwanninger M, Kant M, Schuurink R, Mauch F, et al** (2007) The PP2C-type phosphatase AP2C1, which negatively regulates MPK4 and

MPK6, modulates innate immunity, jasmonic acid, and ethylene levels in *Arabidopsis*. Plant Cell **19:** 2213–2224

**Shin H, Shin HS, Guo Z, Blancaflor EB, Masson PH, Chen R** (2005) Complex regulation of Arabidopsis AGR1/PIN2-mediated root gravitropic response and basipetal auxin transport by cantharidin-sensitive protein phosphatases. Plant J **42:** 188–200

**Slabas AR, Fordham-Skelton AP, Fletcher D, Martinez-Rivas JM, Swinhoe R, Croy RRD, Evans IM** (1994) Characterisation of cDNA and genomic clones encoding homologues of the 65 kDa regulatory subunit of protein phosphatase 2A in *Arabidopsis thaliana*. Plant Mol Biol **26:** 1125–1138

**Sokolov LN, Dominguez-Solis JR, Allary AL, Buchanan BB, Luan S** (2006) A redox-regulated chloroplast protein phosphatase binds to starch diurnally and functions in its accumulation. Proc Natl Acad Sci USA **103:** 9732–9737

**Song SK, Clark SE** (2005) POL and related phosphatases are dosage-sensitive regulators of meristem and organ development in Arabidopsis. Dev Biol **285:** 272–284

**Stepanova AN, Hoyt JM, Hamilton AA, Alonso JM** (2005) A link between ethylene and auxin uncovered by the characterization of two root-specific ethylene-insensitive mutants in *Arabidopsis*. Plant Cell **17:** 2230–2242

**Stone JM, Trotochaud AE, Walker JC, Clark SE** (1998) Control of meristem development by CLAVATA1 receptor kinase and kinase-associated protein phosphatase interactions. Plant Physiol **117:** 1217–1225

**Testerink C, Dekker HL, Lim ZY, Johns MK, Holmes AB, Koster CG, Ktistakis NT, Munnik T** (2004) Isolation and identification of phosphatidic acid targets from plants. Plant J **39:** 527–536

**Tian GW, Mohanty A, Chary SN, Li S, Paap B, Drakakaki G, Kopec CD, Li J, Ehrhardt D, Jackson D, et al** (2004) High-throughput fluorescent tagging of full-length Arabidopsis gene products in planta. Plant Physiol **135:** 25–38

**Ulm R, Ichimura K, Mizoguchi T, Peck SC, Zhu T, Wang X, Shinozaki K, Paszkowski J** (2002) Distinct regulation of salinity and genotoxic stress responses by Arabidopsis MAP kinase phosphatase 1. EMBO J **21:** 6483–6493

**van Zyl W, Huang W, Sneddon AA, Stark M, Camier S, Werner M, Marck C, Sentenac A, Broach JR** (1992) Inactivation of the protein phosphatase 2A regulatory subunit A results in morphological and transcriptional defects in *Saccharomyces cerevisiae*. Mol Cell Biol **12:** 4946–4956

**Wei Q, Xia Y** (2006) Proteasome inhibition down-regulates endothelial nitric-oxide synthase phosphorylation and function. J Biol Chem **281:** 21652–21659

**Xing Y, Xu Y, Chen Y, Jeffrey PD, Chao Y, Lin Z, Li Z, Strack S, Stock JB, Shi Y** (2006) Structure of protein phosphatase 2A core enzyme bound to tumor-inducing toxins. Cell **127:** 341–353

**Yoshida T, Nishimura N, Kitahata N, Kuromori T, Ito T, Asami T, Shinozaki K, Hirayama T** (2006) ABA-hypersensitive germination3 encodes a protein phosphatase 2C (AtPP2CA) that strongly regulates abscisic acid signaling during germination among Arabidopsis protein phosphatase 2Cs. Plant Physiol **140:** 115–126

**Yu RM, Zhou Y, Xu ZF, Chye ML, Kong RY** (2003) Two genes encoding protein phosphatase 2A catalytic subunits are differentially expressed in rice. Plant Mol Biol **51:** 295–311

**Yu S, Lei H, Chang W, Söll D, Hong G** (2001) Protein phosphatase 2A: identification in *Oryza sativa* of the gene encoding the regulatory A subunit. Plant Mol Biol **45:** 107–112

**Zhou HW, Nussbaumer C, Chao Y, DeLong A** (2004) Disparate roles for the regulatory A subunit isoforms in *Arabidopsis* protein phosphatase 2A. Plant Cell **16:** 709–722

**Zhou J, Pham HT, Ruediger R, Walter G** (2003) Characterization of the Aalpha and Abeta subunit isoforms of protein phosphatase 2A: differences in expression, subunit interaction, and evolution. Biochem J **369:** 387–398